Azerbaijani Astronomical Journal AAJ **20(2)**, 21–24 (2025) Preprint 4 December 2025 https://doi.org/10.59849/2078-4163.2025.2.21

Description of the helio-geophysical conditions during the magnetically disturbed period of june 21–26, 2015

S. N. Mukasheva[1*], A. B. Andreyev [2], V. I. Kapytin [2], O. I. Sokolova[2], G. B. Tileu[1]

[1] *Al-Farabi Kazakh National University, Faculty of Physics and Technology, Almaty, Kazakhstan*
[2] *Ionosphere Institute, Almaty, Kazakhstan*

Last updated 2025 October 23; in original form 2025 November 25

ABSTRACT

Extreme solar events, such as flares accompanied by coronal mass ejections (CMEs), perturb the Earth's magnetic field and generate fluctuating currents in the ionosphere and magnetosphere. In this study, we describe the helio-geophysical conditions during the magnetically disturbed period of 21–26 June 2015 on the basis of satellite and ground-based observations. Variations in the solar wind, interplanetary magnetic and electric fields, the planetary Kp index, and geomagnetic field components measured at a mid-latitude observatory are analysed. The storm of 22–24 June 2015 represents one of the strongest geomagnetic disturbances of Solar Cycle 24 and provides an important example of a geoeffective CME.

Key words: stars: coronal mass ejections – magnetic field – magnetic storm

1 INTRODUCTION

Extreme solar events, such as flares accompanied by powerful coronal mass ejections (CMEs), perturb the terrestrial magnetic field and generate highly variable currents in the ionosphere and magnetosphere. Geoeffective CMEs influence the entire Sun–interplanetary medium–magnetosphere–ionosphere–atmosphere–Earth system (e.g. Chernogor & Rozumenko 2008; Chernogor 2011).

The scientific interest in such events is driven by their impact on satellite navigation, communication systems, and spacecraft operating in low and medium Earth orbits. A CME directed toward Earth can disrupt both ground-based and space-based technological systems (Afraimovich et al. 2003; Andreyev et al. 2023). Multiple studies have investigated extreme space-weather events of recent solar cycles (e.g. Polekh et al. 2017; Singh & Sripathi 2017; Shpynev et al. 2018; Paul et al. 2020; Chernogor et al. 2020, 2021; Tulasi Ram et al. 2024; Paul et al. 2025; Gordiyenko et al. 2025).

Here, we perform a detailed analysis of helio-geophysical parameters during a very large geomagnetic storm with a sudden commencement that occurred on 22–24 June 2015.

2 MATERIAL AND METHODS

We used 5-min resolution solar wind and interplanetary data provided by OmniWeb (NASA/GSFC; omniweb.gsfc.nasa.gov), as well as planetary geomagnetic indices (Kp) from WDC Kyoto (wdc.kugi.kyoto-u.ac.jp). Local geomagnetic field measurements were obtained from the Alma-Ata Observatory (code AAA; 43.25°N, 76.92°E), part of the INTERMAGNET network.

3 OBSERVATIONAL RESULTS

Using the example of a very large geomagnetic storm with a sudden onset on 22–24 June 2015, we describe the helio-geophysical conditions that led to the occurrence of geomagnetically induced currents at mid-latitudes. Previous studies have carried out a comprehensive analysis of this unique event using measurements from orbiting satellites and ground-based observatories (e.g. Singh & Sripathi 2017; Astafyeva et al. 2016; Baker et al. 2016; Reiff et al. 2016; Piersanti et al. 2017; Zhao et al. 2017; Gopalswamy et al. 2018; Augusto et al. 2018). The novelty of the present work is that we examine this storm from the viewpoint of the variability of solar-wind parameters and interplanetary electric and magnetic fields, and we also present the corresponding variations of geomagnetic-field parameters based on observations from a mid-latitude geomagnetic station.

Figure 1 presents the variations of helio-geophysical parameters from 21 to 25 June 2015. Panel (a) shows the solar-wind dynamic pressure, P (nPa); panel (b) shows the solar-wind speed, SW (km,s^{-1}); panel (c) shows the B_z component of the interplanetary magnetic field (IMF B_z, nT); panel (d) shows the E_y component of the interplanetary electric field

* Contact e-mail: snmukasheva@gmail.com

(IEF E_y, mV,m^{-1}); panel (e) shows the auroral electrojet index, AE (nT); panel (f) shows the eastern electrojet AU (nT, purple) and western electrojet AL (nT, dark green); panel (g) shows the Sym-H index (nT); and panel (h) shows the planetary Kp index.

The AU index (auroral upper) represents the maximum positive deviation of the H component of the geomagnetic field from the quiet-time average across all auroral-zone observatories. The AL index (auroral lower) corresponds to the maximum negative deviation at the same stations. The AT index is defined as the sum of the absolute values of AU and AL, representing the total magnitude of magnetic fluctuations in the H component. The AE index provides a measure of the overall magnetic disturbance in the auroral zone (**?**). The Sym-H index characterizes the symmetric component of the ring current and is commonly used to quantify geomagnetic disturbances at mid-latitudes.

Two solar flares, classified as M2.0 and M2.6, were accompanied by coronal mass ejections (CMEs) directed towards the Earth. The first CME arrived at the Earth's magnetosphere at 05:45 UT on 22 June 2015, causing a modest increase in the Sym-H index of approximately 35 nT. The second CME reached the magnetosphere at 18:30 UT, coinciding with an increase in solar-wind dynamic pressure from 5 to 58 nPa (Fig. 1a) and an increase in solar-wind speed from 350 to 745 km,s^{-1} (Fig. 1b). The onset of the geomagnetic storm is marked by a sudden rise in the Sym-H index of 77 nT at 18:35 UT on 22 June, followed by a sharp decrease to a minimum of 207 nT at 04:25 UT on 23 June. The interval from 18:35 UT on 22 June to 04:25 UT on 23 June corresponds to the main phase of the storm, followed by a slower recovery phase, with Sym-H reaching approximately −60 nT by 00:00 UT on 25 June 2015.

The B_z component of the interplanetary magnetic field (IMF) turned sharply southward, reaching a minimum of −37 nT at 19:20 UT, before returning northward at 19:50 UT (Fig. 1c). The IMF B_z remained predominantly northward, except for a brief interval near 21:00 UT when it turned negative for approximately 20 min (Astafyeva et al. 2016). Under quiet conditions, variations of the interplanetary electric field (IEF) E_y component are typically within 0 ± 0.28 mV,m^{-1}. Following the arrival of the second CME at the Earth's magnetosphere, E_y increased sharply to 25.79 mV,m^{-1} and subsequently varied in antiphase with IMF B_z (Fig. 1d).

After 00:00 UT on 24 June 2015, the IMF B_z and IEF E_y returned to quiet levels. Variations in the AE auroral electrojet index indicate that the storm was accompanied by intense auroral activity, with AE exceeding 2000 nT at 18:30–18:40 UT and again at 20:00–20:30 UT. During the initial phase of the geomagnetic storm associated with the second CME, the AU and AL indices reached maxima of 1265 nT and −1370 nT, respectively, and varied in antiphase throughout the main phase of the storm (Fig. 1f). The Kp index reached a value of 8, identifying the geomagnetic disturbance of 22–23 June as a major solstice storm of Solar Cycle 24 Augusto et al. (2018). Figure 2 shows the variations of the X-, Y-, and Z-components, as well as the total vector

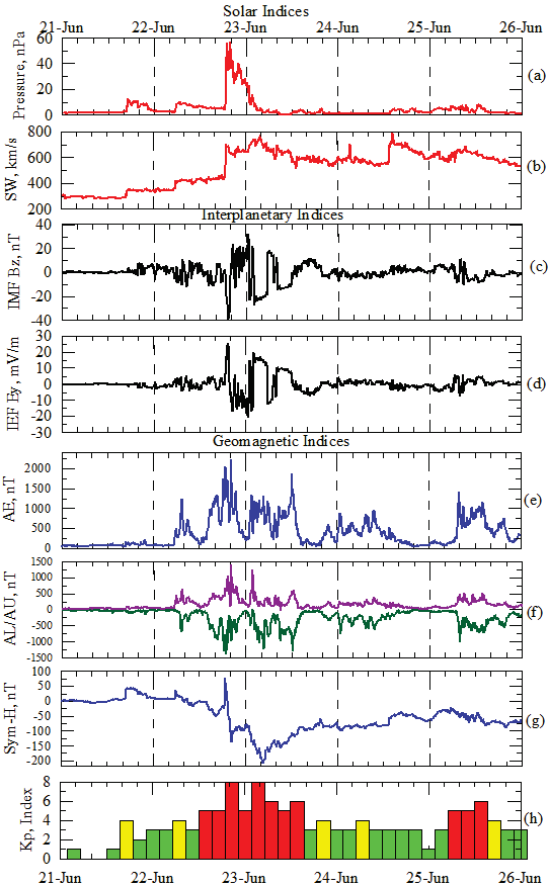

Figure 1. Variation of solar, interplanetary & geomagnetic indices during 21–26 June 2015.

F of the geomagnetic field, based on data from the Alma-Ata Geomagnetic Observatory (code AAA).

The Alma-Ata Geomagnetic Observatory is situated at an altitude of 1300 m in the foothills of the Tien Shan Mountains, approximately 10 km from Almaty, Kazakhstan, with geographic coordinates 43.10°N, 76.57°E, and geomagnetic coordinates 34.3°N, 152.7°E. Geomagnetic measurements are performed using a fluxgate magnetometer (LEMI-008), a portable single-component magnetometer (LEMI-203), and a processor-based Overhauser sensor (POS-1), all conforming to modern international standards. In 2005, the observatory was awarded a quality certificate by the International INTERMAGNET organization.

The observatory measures the X (north), Y (east), and Z (vertical) components of the geomagnetic field vector, as well as the total field F, all in nT. Variations in the XYZ components are recorded at 1 s intervals, while F is sampled every 5 s. Minute-averaged XYZF files are generated from real-time

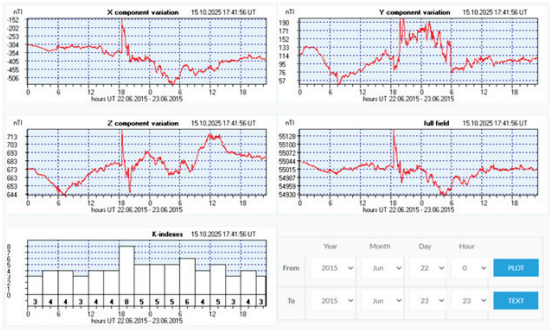

Figure 2. Variations of the X-, Y-, and Z-components of the total geomagnetic field vector, based on data from the Alma-Ata Geomagnetic Observatory, Kazakhstan (observatory code: AAA; coordinates: 43.25°N, 76.92°E).https://ionos.kz/geomagnetic-observatory/

data, and absolute measurements are performed two to three times per week.

Data from 2004 to the present are available through the INTERMAGNET website[1]. Historical local data from 1964–2003 (hourly HDZF) and 2003–present (second- and minute-resolution XYZF) can be provided upon request. The Institute of Ionosphere offers open access to minute- and hourly-averaged XYZF data and K-index values from 2003 onwards.

The mid-latitude geomagnetic observatory AAA recorded a very large geomagnetic storm with a sudden commencement (SC) during the period from 17:40 UT on June 21, 2015, to 21:00 UT on June 25, 2015, lasting 101 hours and 20 minutes. The maximum local K-index reached 8, and the minimum value of the X-component, −544.8 nT, was observed at 04:51:00 UT on June 23, 2015 (Fig. **??**).

4 CONCLUSION

Based on satellite and ground-based observations, we have described the helio-geophysical conditions during the magnetically disturbed period of 21–26 June 2015. Accounting for these conditions is essential for modelling variations of electromagnetic fields in near-Earth space. The variability of parameters during geoeffective coronal mass ejections must be considered in space weather forecasting to mitigate the adverse effects of the radiation environment on both spacecraft instrumentation and ground-based technological systems.

During geomagnetic storms, corpuscular eruptions occur, predominantly involving electrons and protons from the Earth's radiation belts. Eruptions of energetic charged particles from the magnetosphere and radiation belts can contribute to longitudinal currents, but the principal effect of these eruptions on geomagnetically induced currents (GICs) follows a well-understood mechanism. Particles with kiloelectronvolt energies precipitating into the ionosphere enhance ionization at altitudes of 90–120 km, increasing conductivity in affected regions. According to Ohm's law, this leads to amplified horizontal ionospheric currents and associated magnetic fields. Temporal variations of these fields, particularly during storms and sub-storms, induce GICs in pipelines and power systems via Faraday's law (Andreyev et al. 2023). Future work will focus on the effects of extreme solar events in the upper layers of the Earth's atmosphere.

This study provides a useful reference for researchers in solar–terrestrial physics and offers methodological guidance for undergraduate, master's, and doctoral students analysing helio-geophysical data.

[1] www.intermagnet.org

AUTHOR CONTRIBUTIONS

All authors contributed to the conception and design of the study. Material preparation, data collection, and analysis were performed by S. N. Mukasheva, A. B. Andreyev, V. I. Kapytin, O. I. Sokolova, and G. B. Tileu. The first draft of the manuscript was written by S. N. Mukasheva, and all authors provided critical revisions. All authors have read and approved the final version of the manuscript.

CONFLICT OF INTEREST

The authors state that they have no conflict of interest.

FUNDING

This research has been funded by the Science Committee of the Ministry of Science and Higher Education of the Republic of Kazakhstan (Grant No. AP26103851).

REFERENCES

Afraimovich, E. L., Demyanov, V. V., & Kondakova, T. N., 2003, PS Solut., **7**, 109
Andreyev, A. B., Mukasheva, S. N., Kapytin, V. I., & Sokolova, O. I., 2023, Space Weather, **21**, e2023SW003639
Astafyeva, E., Zakharenkova, I., & Alken, P., 2016, Earth Planet. Space, **68**, 152
Augusto, C. R. A., Navia, C. E., & de Oliveira, M. N., 2018, Sol. Phys., **293**, 5
Bailey, R. L., Leonhardt, R., Möstl, C., Beggan, C., Reiss, M. A., Bhaskar, A., & Weiss, A. J., 2022, Space Weather, **20**, e2021SW002907
Baker, D. N., Jaynes, A. N., Kanekal, S. G., et al., 2016, JGR Space Physics, **121**, 6647
Chernogor, L. F., & Rozumenko, V. T., 2008, Radio Phys. Radio Astron., **13**, 120
Chernogor, L. F., 2011, Int. J. Rem. Sens., **32**, 3199
Chernogor, L. F., Garmash, K. P., et al., 2020, Adv. Space Res., **66**, 226
Chernogor, L. F., Garmash, K. P., Guo, Q., et al., 2021, Geomagn. Aeron., **61**, 73

Ebihara, Y., Watari, S., & Kumar, S., 2021, Earth Planets Space, **73**, 163
Gopalswamy, N., Mkel, P., et al., 2018, J. Atmos. Sol. Terr. Phys., **179**, 225
Gordiyenko, G., Arikan, F., Litvinov, Y., & Zhiganbaev, M., 2025, Atmosphere, **16**, 854
Kane, R. P., 2005, Adv. Space Res., **35**, 866
Paul, B., Gordiyenko, G., & Galav, P., 2020, Astrophys. Space Sci., **365**, 174
Paul, K. S., Haralambous, H., Moses, M., & Tripathi, S. C., 2025, Remote Sens., **17**, 2329
Piersanti, M., Alberti, T., Bemporad, A., et al., 2017, Sol. Phys., **292**, 169
Polekh, N., Zolotukhina, N., Kurkin, V., Zherebtsov, G., Shi, J., Wang, G., & Wang, Z., 2017, Adv. Space Res., **60**, 2464
Reiff, P. H., Daou, A. G., & K. J., 2016, Geophys. Res. Lett., **43**, 7311
Sibeck, D. G., Lopez, R. E., & Roleof, E. C., 1991, J. Geophys. Res., **96**, 5489
Singh, R., & Sripathi, S., 2017, J. Geophys. Res. Space Phys., **122**, 11645
Shpynev, B. G., Zolotukhina, N. A., et al., 2018, J. Atmos. Sol.-Terr. Phys., **180**, 93
Tulasi Ram, S., Veenadhari, B., et al., 2024, Space Weather, **22**, e2024SW004126
Zhao, X., Liu, Y. D., Hu, H., & Wang, R., 2017, Astrophys. J., **837**, 10